# Image Segmentation Based on Adaptive Mode Quantization and 2D Histograms Analysis

**Article** · March 2020

CITATIONS
5

READS
53

**2 authors:**

Roumen Kirilov Kountchev
Technical University of Sofia
**268** PUBLICATIONS **663** CITATIONS
SEE PROFILE

Roumiana Kountcheva
TK Engineering, Bulgaria, Sofia
**159** PUBLICATIONS **435** CITATIONS
SEE PROFILE

# Image Segmentation Based on Adaptive Mode Quantization and 2D Histograms Analysis

ROUMEN KOUNTCHEV
Radio Communications and Video Technologies
Technical University - Sofia
Bul. Kl. Ohridsky 8, Sofia
BULGARIA
rkountch@tu-sofia.bg; http://www.tu-sofia.bg

ROUMIANA KOUNTCHEVA
T&K Engineering

Mladost 3, Pb. 12, 1712
BULGARIA
kountcheva_r@yahoo.com

*Abstract:* - In the paper is presented a new method for segmentation of halftone images, based on adaptive quantization of the generalized one-dimensional histogram modes obtained through analysis of the oriented 2D histograms and double nonlinear grey level transform. Specific for the method is that it does not use thresholds defined through iterative analysis of the image histogram which are characteristic for the famous threshold segmentation methods. The new approach permits hierarchical image segmentation through reduction of the grey levels number in the initial hierarchical level. In each consecutive segmentation level the number of grey levels is increased, until the maximum is got. The method is illustrated by an example which shows higher segmentation accuracy, when compared to the well-known iterative Otsu method based on thresholds calculated through one-dimensional histogram analysis. The high accuracy and the low computational complexity of the presented method open new possibilities for real-time applications in the contemporary computer vision systems.

*Key-Words:* - image segmentation, adaptive quantization of the one-dimensional histogram modes, oriented 2D histograms, multiple grey-level transform.

## 1 Introduction

The segmentation is usually used to divide the image into non-overlapping areas characterized by common qualities, for example - same or close grey scale value for all pixels in one region. The famous methods for image segmentation [1,2,3] could be classified as follows: region segmentation; contour segmentation and texture segmentation.

In this work is offered new method for halftone image segmentation, related to the first group. In this case, the segmented image contains homogenous areas, where the pixels of each region have same grey level.

Large number of methods and algorithms for segmentation of halftone images are already known, based on threshold selection which use the grey-level one-dimentional (1D) histogram, such as: the optimal Bayes thresholding [1], the Otsu thresholding [4, 5], the histogram entropy thresholding [6], the multi-level thresholding using hill climbing [7]; the K-means clustering [3]; the fuzzy c-means clustering [8,9], the multispectral thresholding [3], segmentation based on multi-resolution analysis and wavelets [10], etc. Large number of well-known segmentation methods are based on the analysis of the two-dimensional (2D) histograms, and on the related co-occurrence matrices [11,12,13]. In [11] is generalized the Otsu method, based on the analysis of the grey-level 2D histograms. In [12], a method for color image segmentation is offered through 2D histograms analysis in the HSV space, and in [13] the co-occurrence matrices are used as a basis for human face recognition.

The new method is distinguished by the use of adaptive quantization of the modes of the generalized 1D histogram, obtained through analysis of the "oriented" 2D histograms and double nonlinear transform of the grey levels of the processed halftone image.

The basics of the method are given in Section 2; in Section 3 is shown how the segmentation accuracy is enhanced through the analysis of the oriented 2D histograms; in Section 4 is introduced a numerical example for image segmentation; in Section 5 the method is generalized for hierarchical segmentation, and the last section comprises the conclusions, and the future work trends.

## 2 Basic Segmentation Method

### 2.1 Basic idea of the method

The segmentation method, presented here, is based on the use of the 1D histogram of the halftone image, called initial. The basic idea is to detect the positions of the modes in the histogram on the basis of which

to be executed the image segmentation. For this, here is used adaptive histogram mode quantization.

To perform the segmentation, two functions for adaptive transform of the pixels brightness level are calculated. The first is got through the equalization of the initial histogram, and the second - through the equalization of the histogram of the segmented image got in result of the adaptive quantization of the modes of the initial histogram. These two functions, represented as look-up-tables (LUT), are used for the double adaptive non-linear transform of the halftone image pixels brightness, in result of which is obtained the segmented image. To increase the segmentation accuracy, second segmentation is executed for all detached pixels whose grey levels are different from these of their neighbors. The new levels for the detached pixels are calculated on the basis of these of the surrounding pixels, in accordance with the "majority rule" (higher than 50%). The further enhancement of the segmentation accuracy is based on the analysis of the image 2D histograms which represent the frequency of appearance of the couples of neighboring pixels in four directions: horizontal, vertical and both diagonals. The analysis of the "oriented" 2D histograms enables the detection of the „hidden" modes in the initial image histogram. For this are calculated the projected 1D histograms calculated from the matrices of the four basic 2D histograms after their projection in horizontal and vertical directions. Each projected 1D histogram is defined through summation of the elements in the rows and columns of the matrix of the corresponding 2D histogram. From these four projected 1D histograms is calculated the generalized projected 1D histogram, as a median of the arguments of the four histograms. The use of the generalized histogram instead of the initial, results into higher segmentation accuracy because errors due to possible "hidden" modes in the initial histogram, are less. "Hidden" are the modes in the 2D histogram, which do not appear in the projected 1D histogram because they are overlapped by other modes. The final segmented image consists of homogenous areas which correspond to areas of low dispersion in the initial image, in respect to their mean grey level.

## 2.2 Basic steps of the method

The method comprises 7 basic steps:

***Step 1***. The 1D histogram of the halftone image is calculated in accordance with the relation: $h_{in}(k) = n(k)/S$ for k=0,1,..,L-1 where n(k) is the number of pixels whose grey level is k; L is the number of the discrete grey levels for each pixel ($L=2^l$), and S is the total number of pixels.

***Step 2.*** Adaptive quantization of the modes of the histogram $h_{in}(k)$ is executed. For this is defined the staircase-like function $g_1(k)$, used for the LUT transform (LUT-1), in correspondence with the relation:

$$g_1(k)=\begin{cases}\beta_1, & \text{if } h_{in}(\beta_1)=\max \text{ for } 0 \le \beta_1 < \alpha_1,\\ \beta_i, & \text{if } h_{in}(\beta_i)=\max \text{ for } \alpha_{i-1} \le \beta_i < \alpha_i,\ i=2,3,..,m.\end{cases} \quad (1)$$

Here $\alpha_i$ and $\beta_i$ define the positions of the local minimums and maximums (i.e., the modes) of the function $g_1(k)$, and m is the number of the local maximums. However, in case that the grey level k of the pixel is in the range $(\alpha_{i-1},\alpha_i)$ where the function $g_1(k)$ has n identical maximum values, i.e., $g_1(k_1)=g_1(k_2)=\ldots=g_1(k_n)=\max$. The value of $\beta_i$ is calculated as the mean value of the initial and the end level ($k_1$ and $k_n$ correspondingly) of the range, i.e., $\beta_i=(1/2)(k_1+k_n)$. In similar way, if k is in the range $(\beta_{i-1},\beta_i)$ where the function $g_1(k)$ has n identical minimum values, we get the relation $g_1(k_1)=g_1(k_2)=\ldots=g_1(k_n)=\min$, and in this case $\alpha_i=(1/2)(k_1+k_n)$.

***Step 3.*** The modes $\beta_i$ of the histogram $h_{in}(k)$ with corresponding areas $S_i$, which are lower than the predefined threshold $\delta_1$, are merged with their closest modes $\beta_{i+1}$, whose areas $S_{i+1}$ are above the threshold $\delta_1$, and are displaced at a distance $|\beta_{i+1}-\beta_i| < \delta_2$ where $\delta_2$ is a second threshold. In result is obtained the modified function $g_{1mod}(k)$ used in the ($LUT\text{-}1_{mod}$) for the level k of $g_{1mod}$, in accordance with the rule (2):

$$g_{1mod}(k)=\beta_{i+1} \text{ for } S_{i\,new}=S_i \cup S_{i+1}, \text{ if}$$

$$S_i=\sum_{l=\alpha_{i-1}}^{\alpha_i} h_{in}(l) \le \delta_1,\ S_{i+1}=\sum_{l=\alpha_i+1}^{\alpha_{i+1}} h_{in}(l) > \delta_1 \text{ and } |\beta_{i+1}-\beta_1| \le \delta_2$$

for i=2,3,..,m-2;

$$g_{1mod}(k)=\beta_2 \text{ for } S_{1\,new}=S_1 \cup S_2, \text{ if}$$

$$S_1=\sum_{l=0}^{\alpha_1} h_{in}(l) \le \delta_1,\ S_2=\sum_{l=\alpha_1+1}^{\alpha_2} h_{in}(l) > \delta_1 \text{ and } |\beta_2-\beta_1| \le \delta_2;$$

$$g_{1mod}(k)=\beta_{m-1} \text{ for } S_{m\text{-}1\,new}=S_{m-1} \cup S_m, \text{ if}$$

$$S_{m-1}=\sum_{l=\alpha_{m-2}}^{\alpha_{m-1}-1} h_{in}(l) > \delta_1 \text{ and } S_m=\sum_{l=\alpha_{m-1}}^{\alpha_m=L-1} h_{in}(l) \le \delta_1 \text{ and } |\beta_m-\beta_{m-1}| \le \delta_2$$

In case that the merging conditions for the neighbor modes are not satisfied, then $g_{1mod}(k)=g_1(k)$. After each merging the modes number is reduced by one, starting from the initial value, m. The values of the thresholds $\delta_1$ and $\delta_2$ are chosen experimentally, on the basis of the preceding segmentation analysis for the investigated image class. From Eqs. (1) and (2) it follows, that the histogram $h_s(k)$ of the transformed image will contain non-zero values for the levels

$k=\beta_1,\beta_2,..,\beta_m$ only. In this case, in result of the used table transform (Eq. 2) is obtained the segmented image, whose segments contain pixels of same grey level $\beta_i$ for i=1,2,..,m.

***Step 4***. The histogram $h_s(k)$ of the segmented image is transformed in accordance with the equalization method used in [1]. For this, the level k of each pixel in the segmented image is calculated using the staircase-like table transform (LUT-2) (3):

$$g_2(k)=(L-1)\sum_{l=0}^{k} h_s(l)=\begin{cases} 0 & \text{for } 0 \le k < \beta_1, \\ (L-1)\sum_{s=1}^{i} S_s & \text{for } \beta_{i-1} \le k < \beta_i,\ i=2,..,m-1, \\ L-1 & \text{for } \beta_m \le k < L-1, \end{cases}$$

where $h_s(k) = n_s(k)/S$ is the histogram of the segmented image; $n_s(k)$ is the number of pixels with value k, and S is the total number of pixels in the image.

***Step 5.*** The initial histogram $h_{in}(k)$ of the processed image is equalized by using relations in accordance with the next table transform (LUT-3):

$$g_3(k) = (L-1)\sum_{l=0}^{k} h_{in}(l) \quad \text{for } k = 0,1,..,L-1, \qquad (4)$$

***Step 6.*** On the pixels with grey level value k is applied second nonlinear transform, so that to obtain segmented image whose histogram is $h_s(k)$. Here, the relation between the transformed grey level r and its value k before the table transform, is defined by the relation $g_3(k) = g_2(r)$, from which it follows that:

$$r=g_2^{-1}[g_3(k)]=g_2^{-1}[(L-1)\sum_{l=0}^{k} h_{in}(l)] \quad \text{for } k=0,1,..,L-1. \qquad (5)$$

In result of the double transform (Eq. 5) the grey level value k of each pixel is substituted by the value r, and the segmented image is obtained. In case that the conditions from Eq. 2 for the modification of the function $g_1(k)$ are not satisfied, the pixels with grey level value r in the segmented image will get one of the m+1 values below:

$$r=\begin{cases} \beta_1 & \text{for } g_3(0) \le g_3(k) \le g_3(\alpha_1), \\ \beta_i & \text{for } g_3(\alpha_{i-1}) < g_3(k) \le g_3(\alpha_i),\ i=2,..,m-1, \\ \beta_m & \text{for } g_3(\alpha_{m-2}) < g_3(k) \le g_3(\alpha_{m-1}), \\ L-1 & \text{for } g_3(\alpha_{m-1}) < g_3(k) \le L-1. \end{cases} \qquad (6)$$

***Step 7.*** Second segmentation is executed for the detached pixels which remained in the segmented image. For this, each detached pixel (i, j) whose grey level $f_s(i, j)$ differs from that of the 8 neighbors $f_s(i+p, j+q)$ for $p,q=0,\pm1$ and $p=q\neq0$, is given the grey level of the pixels $f_s(i+p_0, j+q_0)$, whose number $n_{f_s(i+p_0, j+q_0)}$ is maximum, i.e.:

$$f_s(i, j)=f_s(i+p_0, j+q_0) \text{ for } n_{f_s(i+p_0, j+q_0)}=\max, \quad \text{if } |f_s(i, j)-f_s(i+p, j+q)| \neq 0 \text{ for } p,q = 0,\pm1. \qquad (7)$$

On Fig. 1, as an example, is graphically represented the method for double transform of the grey level value k of each image pixel, into the corresponding value r from the segmented image for the case when m=3 and the conditions from Eq. 2 for modes merging in the histogram $h_{in}(k)$ are not satisfied.

# 3 Segmentation Accuracy Enhancement

In some cases, the method may not offer sufficient segmentation accuracy. The reason could be the existence of well outlined modes in the oriented 2D histograms of the image which had not been used for the segmentation. Each oriented 2D histogram can be transformed into 1D histogram through projection in various directions: horizontal, vertical and both diagonals. Depending on the modes position in the 2D histograms, it is possible the projected 1D histograms to overlap partially. As a result of the overlapped modes „hiding“, the segmentation errors increase. The analysis of all projection 1D histograms permits to detect the hidden modes, which increases the segmentation accuracy. To solve the problem, each oriented 2D histogram is represented as a matrix of size L×L with elements $h_{in}$ (k,p), defined by the relation:

$$h_{in}(k, p) = n(k, p)/R \quad \text{for } k, p = 0,1,..,L-1. \qquad (8)$$

Here, n(k,p) is the number of existing neighbor pixels couples in the image in horizontal (x), vertical (v) and diagonal (d) directions, with grey level values k and p, and R is the total number of pixels couples in the image. Each pixel participates in two neighbor couples where it is placed on first or on second place. The pixels can be neighbors in horizontal, vertical or diagonal directions (left and right diagonal), and the total number of couples where each pixel participates, is 8. For every kind of neighboring the corresponding "oriented" 2D histogram could be defined, represented by one of the matrices $[H_{in,x}]$, $[H_{in,y}]$, $[H_{in,Ld}]$, $[H_{in,Rd}]$ whose elements are $h_{in,x}(k,p)$, $h_{in,y}(k,p)$, $h_{in,Ld}(k,p)$, and $h_{in,Rd}(k,p)$.

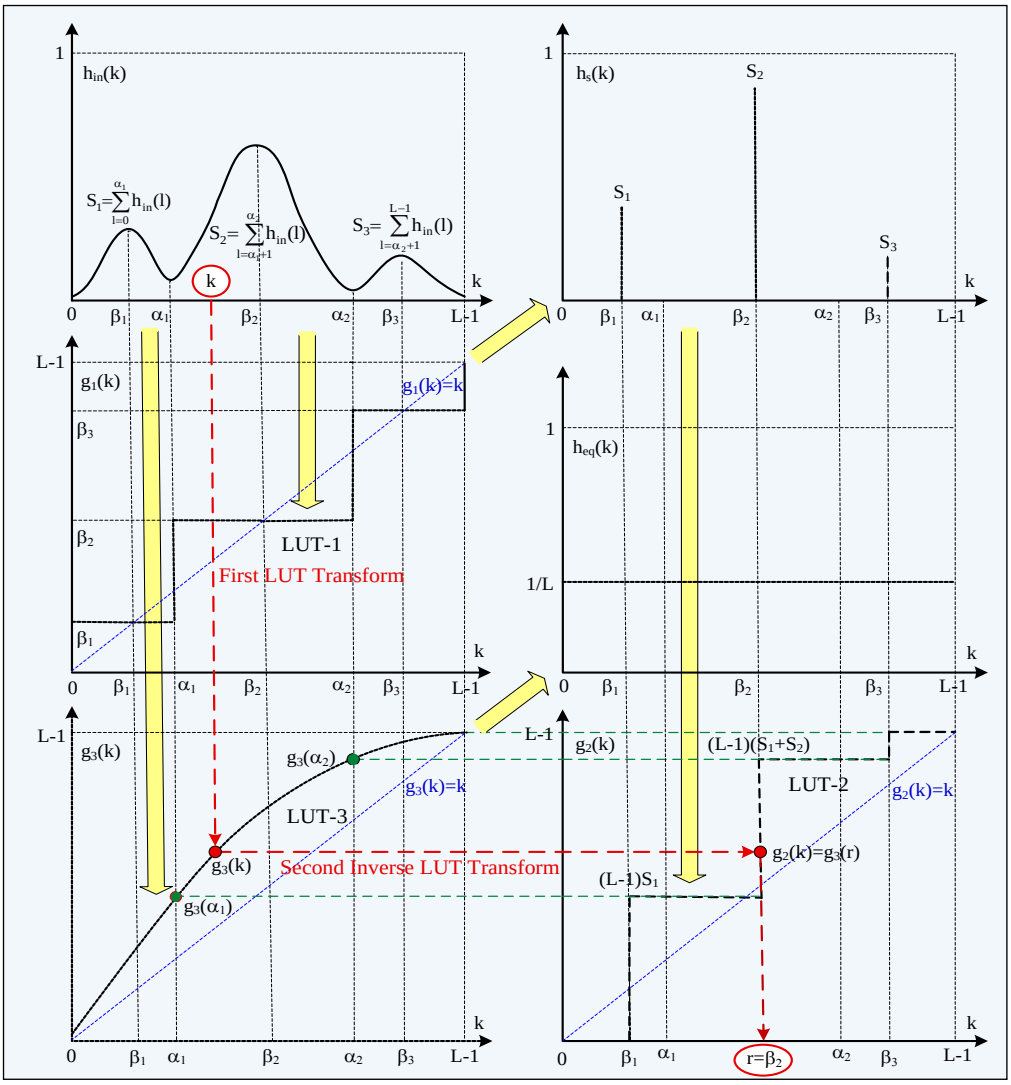


Fig.1. Graphic representation of the adaptive quantization of the histogram $h_{in}(k)$, and double nonlinear transform of the grey level k into r, for k = 0,1,..,L-1.

Through summation of each matrix elements along its columns and rows, are calculated the couples of the projection 1D histograms, respectively: $h_r^x(k)$ and $h_c^x(k)$; $h_r^y(k)$ and $h_c^y(k)$; $h_r^{Ld}(k)$ and $h_c^{Ld}(k)$; $h_r^{Rd}(k)$ and $h_c^{Rd}(k)$. Then, for k,p = 0,1,..,L-1 are got the following eight „oriented“ projected 1D histograms:

$$h_r^x(k)=\sum_{p=0}^{L-1}h_{in,x}(k,p);\quad h_c^x(p)=\sum_{k=0}^{L-1}h_{in,x}(k,p);$$

$$h_r^y(k)=\sum_{p=0}^{L-1}h_{in,y}(k,p);\quad h_r^y(p)=\sum_{k=0}^{L-1}h_{in,y}(k,p); \qquad (9)$$

$$h_r^{Ld}(k)=\sum_{p=0}^{L-1}h_{in,Ld}(k,p);\ h_c^{Ld}(p)=\sum_{k=0}^{L-1}h_{in,Ld}(k,p);$$

$$h_r^{Rd}(k)=\sum_{p=0}^{L-1}h_{in,Rd}(k,p);\ h_r^{Rd}(p)=\sum_{k=0}^{L-1}h_{in,Rd}(k,p).$$

Because of the symmetry of the matrices $[H_{in,x}]$, $[H_{in,y}]$, $[H_{in,Ld}]$ and $[H_{in,Rd}]$ in regard to their main diagonal, the following relations are satisfied:

$$h_r^x(k)=h_c^x(k)=h_{pr}^x(k);\ h_r^y(k)=h_c^y(k)=h_{pr}^y(k);$$
$$h_r^{Ld}(k)=h_c^{Ld}(k)=h_{pr}^{Ld}(k);\ h_r^{Rd}(k)=h_c^{Rd}(k)=h_{pr}^{Rd}(k). \qquad (10)$$

From this it follows, that for each matrix is obtained one projection 1D histogram only, i.e.: $h_{pr}^x(k)$, $h_{pr}^y(k)$, $h_{pr}^{Ld}(k)$ and $h_{pr}^{Rd}(k)$. The combined analysis of the so obtained group of four projection histograms permits to detect the „hidden“ modes in the histogram $h_{in}(k)$, which to be placed in the projections of the oriented 2D histograms. On the basis of the four projection 1D histograms, defined by Eq. 10, could be calculated the median histogram for k=0,1,..,L-1:

$$h_{med}(k)=\text{median}\,[h_{pr}^x(k),h_{pr}^y(k),h_{pr}^{Ld}(k),h_{pr}^{Rd}(k)] \qquad (11)$$

The median histogram can be used as a generalized projection 1D histogram. It can contain new "hidden" modes, which coincide with these of $h_{in}(k)$. To increase the segmentation accuracy through reduction of the errors due to possible "hidden" modes in the histogram $h_{in}(k)$, it is necessary to substitute $h_{in}(k)$ by the generalized histogram $h_{med}(k)$ prior to execution of the described method.

## 4 Numerical Example

On Fig. 2 is shown one example test halftone image of size 8×8 pixels where the grey level values, which are in the range from 0 to 7 (for L=8), are substituted by corresponding pseudo colors.

On Fig. 3 is shown the segmentation result for the image consisting of 64 pixels (S=8×8). All histograms and transform tables (LUT) are graphically represented on Fig. 4.

| | | | | | | | | |
|---|---|---|---|---|---|---|---|---|
| 0 | 1 | 1 | 2 | 1 | 2 | 7 | 7 | 7 |
| 1 | 1 | 3 | 2 | 3 | 2 | 7 | 3 | 3 |
| 2 | 2 | 7 | 7 | 7 | 3 | 2 | 4 | 3 |
| 3 | 1 | 7 | 7 | 1 | 1 | 1 | 6 | 2 |
| 4 | 1 | 2 | 3 | 1 | 1 | 6 | 6 | 1 |
| 5 | 4 | 4 | 4 | 3 | 2 | 6 | 6 | 2 |
| 6 | 2 | 2 | 4 | 3 | 2 | 2 | 1 | 1 |
| 7 | 1 | 1 | 1 | 1 | 2 | 1 | 2 | 1 |

a. Test image of size 8×8 pixels and the scale, used to color the corresponding grey levels

| | | | | | | | |
|---|---|---|---|---|---|---|---|
| 2 | 2 | 4 | 2 | 4 | 7 | 7 | 7 |
| 2 | 5 | 4 | 5 | 4 | 7 | 5 | 5 |
| 4 | 7 | 7 | 7 | 5 | 4 | 5 | 5 |
| 2 | 7 | 7 | 2 | 2 | 2 | 6 | 4 |
| 2 | 4 | 5 | 2 | 2 | 6 | 6 | 2 |
| 5 | 5 | 5 | 5 | 4 | 6 | 6 | 4 |
| 4 | 4 | 5 | 5 | 5 | 4 | 2 | 2 |
| 2 | 2 | 2 | 2 | 4 | 2 | 4 | 2 |

b. The image from Fig. 2a after histogram equalization

Fig. 2. Test image equalization

| | | | | | | | |
|---|---|---|---|---|---|---|---|
| 1 | 1 | 1 | 1 | 1 | 7 | 7 | 7 |
| 1 | 1 | 1 | 1 | 1 | 7 | 1 | 1 |
| 1 | 7 | 7 | 7 | 1 | 1 | 1 | 1 |
| 1 | 7 | 7 | 1 | 1 | 1 | 7 | 1 |
| 1 | 1 | 1 | 1 | 1 | 7 | 7 | 1 |
| 1 | 1 | 1 | 1 | 1 | 7 | 7 | 1 |
| 1 | 1 | 1 | 1 | 1 | 1 | 1 | 1 |
| 1 | 1 | 1 | 1 | 1 | 1 | 1 | 1 |

a. The test image segmented on the basis of functions $g_2(k)$ and $g_3(k)$, as given in Table 1

| | | | | | | | |
|---|---|---|---|---|---|---|---|
| 1 | 1 | 2 | 1 | 2 | 7 | 7 | 7 |
| 1 | 2 | 2 | 2 | 2 | 7 | 2 | 2 |
| 2 | 7 | 7 | 7 | 2 | 2 | 2 | 2 |
| 1 | 7 | 7 | 1 | 1 | 1 | 6 | 2 |
| 1 | 2 | 2 | 1 | 1 | 6 | 6 | 1 |
| 2 | 2 | 2 | 2 | 2 | 6 | 6 | 2 |
| 2 | 2 | 2 | 2 | 2 | 2 | 1 | 1 |
| 1 | 1 | 1 | 1 | 2 | 1 | 2 | 1 |

b. The test image segmented on the basis of functions $g_2(k)$ and $g_3(k)$, as given in Table 3

Fig. 3. Image segmentation results

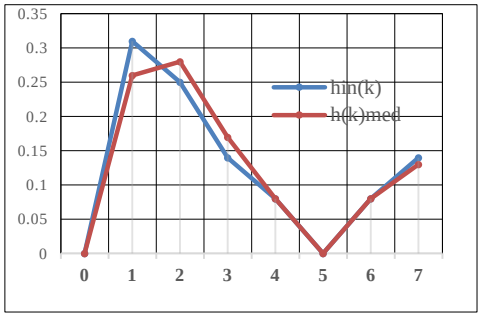


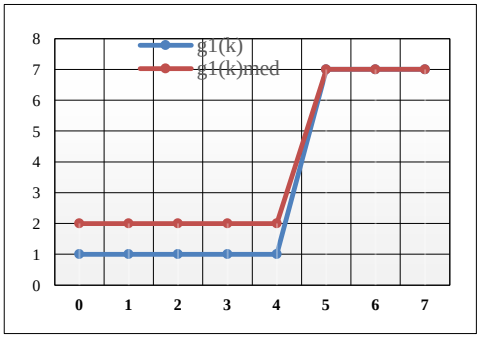


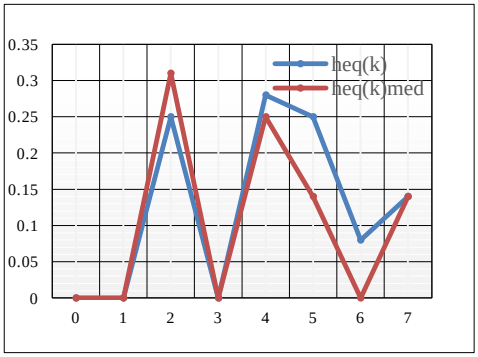


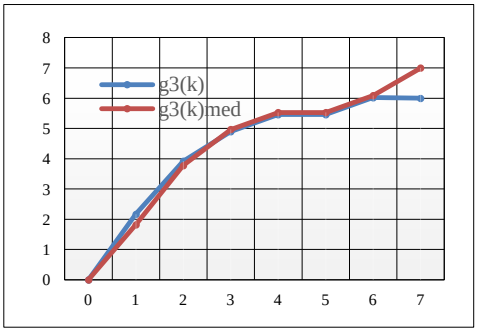

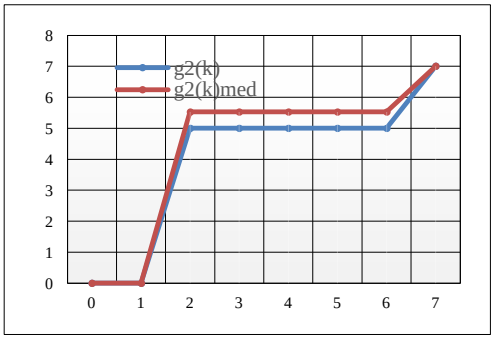


Fig. 4. Graphic representation of histograms $h_{in}(k)$, $h_{eq}(k)$, $h_s(k)$ (blue color), and the transform tables (LUT-1,2,3) represented by the functions $g_1(k)$, $g_2(k)$, $g_3(k)$. The orange graphics are calculated on the basis of the data from Table 2, obtained through analysis of the 2D histograms of the image from Fig. 2 a.

Table 1. Histograms $h_{in}(k)$, $h_{eq}(k)$, $h_s(k)$ and transform functions $g_1(k)$, $g_2(k)$, $g_3(k)$

| k | 0 | 1 | 2 | 3 | 4 | 5 | 6 | 7 |
|---|---|---|---|---|---|---|---|---|
| $h_{in}(k)$ | 0 | **0.31** | 0.25 | 0.14 | 0.08 | 0 | 0.08 | **0.14** |
| $h_{eq}(k)$ | 0 | 0 | **0.25** | 0 | **0.28** | 0.25 | 0.08 | **0.14** |
| $h_s(k)$ | 0 | **0.78** | 0 | 0 | 0 | 0 | 0 | **0.22** |
| $g_1(k)$ | 1 | 1 | 1 | 1 | 1 | 7 | 7 | 7 |
| $g_2(k)$ | 0 | 5 | 5 | 5 | 5 | 5 | 5 | 7 |
| $g_3(k)$ | 0 | 2.17 | 3.92 | 4.9 | 5.46 | 5.46 | 6.02 | 7 |

Table 2. Histograms

| k | 0 | 1 | 2 | 3 | 4 | 5 | 6 | 7 |
|---|---|---|---|---|---|---|---|---|
| $h_{pr}^{x}(k)$ | 0 | **0.28** | **0,28** | 0.17 | 0.07 | 0 | 0.08 | **0.12** |
| $h_{pr}^{y}(k)$ | 0 | **0.29** | 0.25 | 0.18 | 0.07 | 0 | 0.07 | **0.13** |
| $h_{pr}^{Ld}(k)$ | 0 | 0.20 | **0.31** | 0.14 | 0.09 | 0 | 0.10 | **0.15** |
| $h_{pr}^{Rd}(k)$ | 0 | 0.25 | **0.27** | 0.14 | 0.09 | 0 | 0.10 | **0.15** |
| $h_{med}(k)$ | 0 | 0.26 | **0.28** | 0.16 | 0.08 | 0 | 0.09 | **0.13** |
| $h_{in}(k)$ | 0 | **0.31** | 0.25 | 0.14 | 0.08 | 0 | 0.08 | **0.14** |

To perform the segmentation in accordance with the described method are used the three transform functions $g_1(k)$, $g_2(k)$, $g_3(k)$, given in Table 1. The maximums of these functions are written in **bold** in the table. From the analysis of the histogram $h_{in}(k)$ are defined the parameters $\alpha_i$=5, $\beta_1$=2 and $\beta_2$=7. The segmentation is executed for the threshold values: $\delta_1$=0.01 and $\delta_2$=1. In this case, the conditions from Eq. 2 for merging neighboring modes in the histogram $h_{in}(k)$ are not satisfied. The segmentation is done on the basis of Eq. (6) for double transform (substitution) of the value k by the value r, for each pixel. The segmentation result from Fig. 3a shows that the obtained two segments correspond to the background (grey level value "1"), and to the objects (grey level value "7").

On the basis of Eq. (8), for the image shown on Fig. 2a could be calculated four matrices, which represent the corresponding normalized oriented 2D histograms in the directions x, y and along both diagonals: $L_d$ (left) and $R_d$ (right). Each matrix, shown on Fig. 5, is represented as a 2D surface. All elements of the matrices, for which the corresponding discrete surface has local maximums, are marked in **bold**. Through projection of each matrix along their rows and columns, and in accordance to Eqs. (9) - (11), are obtained the projection 1D histograms, given in Table 2. From the comparison of the results from Tables 1 and 2 for the histograms $h_{med}(k)$ and $h_{in}(k)$ could be noticed that the first contains a new mode which does not exist in the initial (second) histogram.

$$[H_{in,x}] = \begin{bmatrix} 0 & 0 & 0 & 0 & 0 & 0 & 0 & 0 \\ 0 & 0.10 & \mathbf{0.11} & 0.02 & 0 & 0 & 0.04 & 0.02 \\ 0 & \mathbf{0.11} & 0.02 & \mathbf{0.08} & 0.01 & 0 & 0.02 & \mathbf{0.04} \\ 0 & 0.02 & \mathbf{0.08} & 0.01 & 0.04 & 0 & 0 & 0.02 \\ 0 & 0 & 0.01 & 0.04 & 0.02 & 0 & 0 & 0 \\ 0 & 0 & 0 & 0 & 0 & 0 & 0 & 0 \\ 0 & 0.04 & 0.02 & 0 & 0 & 0 & 0.02 & 0 \\ 0 & 0.02 & \mathbf{0.04} & 0.02 & 0 & 0 & 0 & 0.04 \end{bmatrix}$$

$$[H_{in,y}] = \begin{bmatrix} 0 & 0 & 0 & 0 & 0 & 0 & 0 & 0 \\ 0 & 0.06 & \mathbf{0.13} & 0.06 & 0.01 & 0 & 0.02 & 0.01 \\ 0 & \mathbf{0.13} & 0,04 & 0.02 & 0.02 & 0 & 0.01 & 0.03 \\ 0 & 0.06 & 0.02 & 0.02 & 0.02 & 0 & 0 & \mathbf{0.06} \\ 0 & 0.01 & 0.02 & 0.02 & 0.01 & 0 & 0.01 & 0 \\ 0 & 0 & 0 & 0 & 0 & 0 & 0 & 0 \\ 0 & 0.02 & 0.01 & 0 & 0.01 & 0 & 0.03 & 0 \\ 0 & 0.01 & 0.03 & \mathbf{0.06} & 0 & 0 & 0 & 0.03 \end{bmatrix}$$

$$[H_{in,R_d}] = \begin{bmatrix} 0 & 0 & 0 & 0 & 0 & 0 & 0 & 0 \\ 0 & 0.01 & \mathbf{0.08} & 0.02 & 0.02 & 0 & \mathbf{0.07} & 0.05 \\ 0 & \mathbf{0.08} & 0.03 & 0.04 & 0.04 & 0 & 0.02 & 0.04 \\ 0 & 0.02 & 0.04 & 0.03 & 0.01 & 0 & 0 & 0.04 \\ 0 & 0.02 & 0.04 & 0.01 & 0.01 & 0 & 0 & 0.01 \\ 0 & 0 & 0 & 0 & 0 & 0 & 0 & 0 \\ 0 & \mathbf{0.07} & 0.02 & 0 & 0 & 0 & 0.01 & 0 \\ 0 & 0.05 & 0.04 & 0.04 & 0.01 & 0 & 0 & 0.01 \end{bmatrix}$$

$$[H_{in,L_d}] = \begin{bmatrix} 0 & 0 & 0 & 0 & 0 & 0 & 0 & 0 \\ 0 & 0.06 & \mathbf{0.08} & 0.02 & 0.02 & 0 & 0.01 & 0.01 \\ 0 & \mathbf{0.08} & 0.01 & \mathbf{0.08} & 0.02 & 0 & \mathbf{0.06} & \mathbf{0.06} \\ 0 & 0.02 & \mathbf{0.08} & 0 & 0.04 & 0 & 0.01 & 0.04 \\ 0 & 0.02 & 0.02 & 0.04 & 0 & 0 & 0 & 0 \\ 0 & 0 & 0 & 0 & 0 & 0 & 0 & 0 \\ 0 & 0.01 & \mathbf{0.06} & 0.01 & 0 & 0 & 0.01 & 0 \\ 0 & 0.01 & \mathbf{0.06} & 0.04 & 0 & 0 & 0 & 0.02 \end{bmatrix}$$

Fig. 5. Matrices of the „oriented“ 2D histograms for the image from Fig. 2a in directions x, y and along both diagonals: $L_d$ and $R_d$.

Table 3. Histograms and transform functions

| k | 0 | 1 | 2 | 3 | 4 | 5 | 6 | 7 |
|---|---|---|---|---|---|---|---|---|
| $h_{med}(k)$ | 0 | 0.26 | **0.28** | 0.16 | 0.08 | 0 | 0.09 | **0.16** |
| $h_{eq}(k)_{med}$ | 0 | 0 | **0.31** | 0 | **0.25** | 0.14 | 0 | **0.14** |
| $h_s(k)_{med}$ | 0 | 0 | **0.79** | 0 | 0 | 0 | 0 | **0.21** |
| $g_1(k)_{med}$ | 2 | 2 | 2 | 2 | 2 | 7 | 7 | 7 |
| $g_2(k)_{med}$ | 0 | 0 | 5.53 | 5.53 | 5.53 | 5.53 | 5.53 | 7 |
| $g_3(k)_{med}$ | 0 | 1.82 | 3.78 | 4.97 | 5.53 | 5.53 | 6.09 | 7 |

Let for the example from Fig. 2 the histogram $h_{in}(k)$ is substituted by $h_{med}(k)$, and after that is executed image segmentation in accordance with the method, given above. Then, on the basis of the histogram $h_{mean}(k)$ are calculated three new transform functions $g_1(k)_{med}$, $g_2(k)_{med}$, $g_3(k)_{med}$, given in Table 3. The segmentation result is shown on Fig. 3b. In this case are obtained four segments with grey level values “1”, “2”, “6” and “7”. The shape of the segments with levels “6” and ”7” corresponds to the shape with level “7” from Fig. 3a, while the segments with levels “1” and “2” comprise the segment with level “1”, as shown on Fig. 3a. The comparison of the original image from Fig. 2a with the corresponding segmented images from Fig. 3a,b (with and without analysis of the “oriented“ 2D histograms) shows that in the second case the segmentation accuracy is increased. In this case, instead of two segments, here were obtained four. The new segments better represent the areas in the original image which have small grey level dispersion in respect of their mean grey values. Let for the example from Fig. 2a is used the "classic" iterative segmentation algorithm of Otsu [4]. Then, if the initial threshold is $\delta_0=2$, the condition to stop the iterations $|\delta_t-\delta_{t-1}|<\varepsilon$ for $\varepsilon=0.5$ is satisfied in the iteration t=3 where the corresponding threshold is $\delta_t=\delta_3=4$. In this case the segmented image has two segments only. The shapes of the segments correspond to these from Fig. 3a, obtained in correspondence with the offered segmentation method based on the 1D histogram of the image, i.e. - without using the “oriented“ 2D histograms.

The investigation of the method efficiency for various groups of test images is still to come. It will permit to evaluate the segmentation accuracy and to compare the obtained results with these of the famous segmentation methods based on iterative histogram analysis.

## 5 Hierarchical Segmentation

To decrease the computational complexity of the offered segmentation algorithm, the number of grey levels is beforehand reduced from $L=2^l$ down to $2^k$ for k<l. As a result, the new image has $2^k$ grey levels only. If the new algorithm is applied on such image, the size of the matrices which represent the normalized oriented 2D histograms are reduced from $2^l\times2^l$ to $2^k\times2^k$ which results in reduction of the size of the average 1D histogram, and of the transform tables $g_1(k)_{med}$, $g_2(k)_{med}$, and $g_3(k)_{med}$, correspondingly. After the execution of the "coarse" segmentation aimed at the detection of the high-contrast areas, it is possible to perform second segmentation (in the areas of interest only) using for them the initial quantization scale of $2^l$ levels. For the example from Fig. 2a after reduction of the grey levels number down to four 4 (for k=2), is got the image shown on Fig. 6a.

| | | | | | | | |
|---|---|---|---|---|---|---|---|
| 0 | 0 | 1 | 0 | 1 | 3 | 3 | 3 |
| 0 | 1 | 1 | 1 | 1 | 3 | 1 | 1 |
| 0 | 3 | 3 | 3 | 1 | 1 | 2 | 1 |
| 0 | 3 | 3 | 0 | 0 | 0 | 3 | 1 |
| 0 | 1 | 1 | 0 | 0 | 3 | 3 | 0 |
| 2 | 2 | 2 | 1 | 1 | 3 | 3 | 1 |
| 1 | 1 | 2 | 1 | 1 | 1 | 0 | 0 |
| 0 | 0 | 0 | 0 | 1 | 0 | 1 | 0 |

a. Image of size 8×8 pixels and with 4 grey levels, represented in pseudo colors;

| | | | | | | | | |
|---|---|---|---|---|---|---|---|---|
| 0 | 0 | 1 | 0 | 1 | 3 | 3 | 3 | 0 |
| 0 | 1 | 1 | 1 | 1 | 3 | 1 | 1 | 1 |
| 0 | 3 | 3 | 3 | 1 | 1 | 2 | 1 | 2 |
| 0 | 3 | 3 | 0 | 0 | 0 | 3 | 1 | 3 |
| 0 | 1 | 1 | 0 | 0 | 3 | 3 | 0 | 4 |
| 2 | 2 | 2 | 1 | 1 | 3 | 3 | 1 | 5 |
| 1 | 1 | 2 | 1 | 1 | 1 | 0 | 0 | 6 |
| 0 | 0 | 0 | 0 | 1 | 0 | 1 | 0 | 7 |

b. The segmented image in accordance with the new method with grey levels multiplied by 2

Fig. 6. Example results. In the right column are shown the used pseudo colors.

The matrices of the normalized oriented 2D histograms are given below:

$$[H_{in,y}]=\begin{bmatrix} 0.10 & \mathbf{0.12} & 0.02 & 0.04 \\ \mathbf{0.12} & 0.10 & 0.05 & \mathbf{0,11} \\ 0.02 & 0.05 & 0.01 & 0.01 \\ 0.04 & \mathbf{0.11} & 0.01 & \mathbf{0.07} \end{bmatrix} \quad [H_{in,x}]=\begin{bmatrix} 0.13 & 0.14 & 0.00 & 0.04 \\ 0.14 & \mathbf{0.16} & 0.04 & \mathbf{0.06} \\ 0.00 & 0.04 & 0.03 & 0.00 \\ 0.04 & \mathbf{0,06} & 0.00 & \mathbf{0.12} \end{bmatrix}$$

$$[H_{in,L_d}]=\begin{bmatrix} 0.06 & 0.09 & 0.05 & 0.08 \\ 0.09 & 0.09 & 0.09 & \mathbf{0.11} \\ 0.05 & 0.09 & 0.00 & 0.00 \\ 0.05 & \mathbf{0.11} & 0.00 & \mathbf{0.07} \end{bmatrix} \quad [H_{in,R_d}]=\begin{bmatrix} 0.04 & 0.13 & 0.01 & \mathbf{0.09} \\ 0.13 & \mathbf{0.14} & 0.05 & \mathbf{0.09} \\ 0.01 & 0.05 & 0.01 & 0.01 \\ \mathbf{0.09} & \mathbf{0.09} & 0.01 & \mathbf{0.04} \end{bmatrix}$$

In Table 4 are given the functions $g_1(k)_{med}$, $g_2(k)_{med}$,$g_3(k)_{med}$ calculated on the basis of histograms $h^x_{pr}(k)$, $h^y_{pr}(k)$, $h^{Ld}_{pr}(k)$ and $h_{med}(k)$.

Table 4. Histograms and transform functions

| k | 0 | 1 | 2 | 3 |
|---|---|---|---|---|
| $h^{x}_{pr}(k)$ | 0.31 | **0.40** | 0.07 | **0.22** |
| $h^{y}_{pr}(k)$ | 0.28 | **0.38** | 0.09 | **0.24** |
| $h^{Ld}_{pr}(k)$ | 0.27 | **0.41** | 0.08 | **0.23** |
| $h^{Rd}_{pr}(k)$ | 0.25 | **0.38** | 0.14 | **0.23** |
| $h_{med}(k)$ | 0.28 | **0.39** | 0.09 | **0.24** |
| $g_1(k)_{med}$ | 1.00 | 1.00 | 1.00 | 3.00 |
| $g_2(k)_{med}$ | 0.00 | 2.28 | 2.28 | 3.00 |
| $g_3(k)_{med}$ | 0.84 | 2.01 | 2.28 | 3.00 |

On Fig. 6b is shown the segmented image got in accordance with the algorithm, and after multiplying the grey level value of each pixel by two. The comparison of the segmented images from Fig. 3b and Fig. 6b shows that the reduction of the grey levels number in this case does not result into change of the shapes of the segmented areas but influences the grey level values in some segments only. For given areas of interest, the segmentation can further continue by applying the algorithm on the pixels from the initial image which are in the corresponding areas.

# 6 Conclusions and Future Work

The presented new method for segmentation of halftone images is in accordance with their statistical qualities, based on the evaluation of the probability density of first and second order, represented by their 1D and 2D grey level histograms. The corresponding segmentation algorithm has low computational complexity and permits to achieve high segmentation accuracy. These advantages permit to define the following basic application areas in the computer vision systems: robotics, automatic analysis of multispectral and hyper spectral images, analysis of medical images, etc.

The future development of the method will be aimed at the investigation of its abilities in:

- hierarchical image segmentation with initially reduced number of grey level values in the first hierarchical level, and second segmentation of each of the segmented areas with consecuentially increasing of the grey level number in the next levels;
- hierarchical image segmentation based on the local histograms of the initially separated blocks;
- parallel execution of the computational operations needed for the method implementation in real-time computer vision systems;
- generalization for 3D images represented as tensors.

***Acknowledgment***

This work was supported by the National Science Fund of Bulgaria: Project No. KP-06-H27/16.

***References***

1. R. Gonzalez, R. Woods. *Digital Image Processing*, 3rd Edition, Prentice Hall, New Jersey, 2008.
2. L. Yaroslavsky, *Digital Picture Processing: An Introduction*, Springer, Berlin, Germany, 1985.
3. P. Ho (Ed.), *Image Segmentation*, InTech Europe Publisher, April 2011.
4. N. Otsu, A threshold selection method from grey-level histograms. *IEEE Trans. Systems Man, and Cybernetics*, Vol. 9, 1979, pp. 62-66.
5. D. Huang, C. Wang, Optimal multi-level thresholding using a two-stage Otsu optimization approach, *Pattern Recognition Letters*, Vol. 30, 2009, pp. 275–284.
6. J. Kapur, P. Sahoo, A. Wong, A new method for gray-level picture thresholding using the entropy of the histogram. *Computer Vision, Graphics, and Image Processing*, Vol. 29, 1985, pp. 273–285.
7. S. Nath, S. Agarwal, Q. Kazmi, Image Histogram Segmentation by Multi-Level Thresholding using Hill Climbing Algorithm, *Intern. Journal of Computer Applications*, Vol. 35, No1, Dec. 2011, pp. 63-72.
8. Y. Yang, S. Huang, Image segmentation by fuzzy c-means clustering algorithm with a novel penalty term, *Computing and Informatics*, Vol. 26, 2007, pp. 17–31.
9. M. Devikar, M. Jha, Segmentation of Images using Histogram based FCM Clustering Algorithm and Spatial Probability, *Intern. Journal of Advances in Engineering & Technology*, March 2013, Vol. 6, Issue 1, pp. 225-231.
10. B. Kim, J. Shim, D. Park, Fast image segmentation based on multi-resolution analysis and wavelets, *Pattern Recognition Letters*, Vol. 24, 2003, pp. 2995–3006.
11. J. Zhang, J. Hu, Image Segmentation Based on 2D Otsu Method with Histogram Analysis, 2008 *Intern. Conference on Computer Science and Software Engineering, IEEE Computer Society*, 2008, pp. 105-108.
12. M. Lhoussaine, Z. Rachid, M. Ansari, Image Segmentation Based on a Two-Dimensional Histogram, Chapter in: *Image Segmentation*, P. Ho (Ed.), InTech Europe Publisher, April 2011, pp. 379-388.
13. A. Eleyan, H. Demirel, Co-occurrence matrix and its statistical features as a new approach for face recognition, *Turk Journal of Elec. Eng & Comp. Sci.*, Vol.19, No.1, 2011, pp. 97-107.